



THE UNIVERSITY *of* EDINBURGH

Edinburgh Research Explorer

Application of the TDD Underlay Concept to Home NodeB Scenario

Citation for published version:

Bharucha, Z & Haas, H 2008, Application of the TDD Underlay Concept to Home NodeB Scenario. in *Proceedings of the Vehicular Technology Conference (VTC 08 - Spring)*.

Link:

[Link to publication record in Edinburgh Research Explorer](#)

Document Version:

Peer reviewed version

Published In:

Proceedings of the Vehicular Technology Conference (VTC 08 - Spring)

General rights

Copyright for the publications made accessible via the Edinburgh Research Explorer is retained by the author(s) and / or other copyright owners and it is a condition of accessing these publications that users recognise and abide by the legal requirements associated with these rights.

Take down policy

The University of Edinburgh has made every reasonable effort to ensure that Edinburgh Research Explorer content complies with UK legislation. If you believe that the public display of this file breaches copyright please contact openaccess@ed.ac.uk providing details, and we will remove access to the work immediately and investigate your claim.



Application of the TDD Underlay Concept to Home NodeB Scenario

Zubin Bharucha and Harald Haas
Institute for Digital Communications
University of Edinburgh
Edinburgh EH9 3JL, UK
Email: {z.bharucha, h.haas}@ed.ac.uk

Abstract—This paper presents a spectrum sharing approach which exploits the clustered distribution of users as would be expected in a typical home with several communicating devices (also known as a femto-cell) or in public places such as airports, malls, etc. From each cluster, a mobile station (MS), known as a gateway mobile (GM), acts as a relay between the other users of the cluster and the base station (BS) of the associated cell. The system makes use of frequency division duplexing (FDD) for communication between the BS and the GM. Traffic is assumed to be asymmetric in favour of downlink (DL) due to current trends in user traffic requirements. The unused resources in the uplink band are then used for communication within the cluster using time division duplexing (TDD underlay). This model is compared against one in which the same user distribution is assumed but the GM concept is not made use of, i.e., an FDD system. Based on the results, it has been shown that the proposed enhancements lead to a significant increase in system spectral efficiency through the use of intra-cluster communication.

I. INTRODUCTION

Due to the poor spectrum utilisation in current wireless networks, a system in which unused resources are exploited is presented as a step towards future wireless network solutions which are envisaged to be characterised by the lack of frequency planning [1]. Dynamic, self-organising and spectrum-sharing networks using picocellular structures are considered as improvements to the current wireless network solutions which do not efficiently utilise the available bandwidth [2], [3].

Ad hoc solutions to cellular networks are becoming more popular. However, all the proposals presented in [4]–[6] either require additional infrastructure to be installed in the system or require complex computations in order to find a suitable route.

Next generation wireless networks face challenges in the form of a highly increased number of users, increased traffic generated by each user and traffic asymmetry in the downlink. Duplexing and resource allocation are two of the critical issues in the design of next generation systems. An air-interface for next generation systems must be efficient and flexible in the utilisation of spectrum and must be able to dynamically allocate resources and exploit multi-user diversity. The hybrid division duplex (HDD) architecture [7] aims to combine the advantages of FDD and TDD schemes to increase the flexibility and efficiency of a mobile communication network. Cell partitioning ensures that nomadic users are provided with high data-rates and asymmetric service through TDD, and high-speed users are given reliable service using FDD. However cell partitioning/sectoring does not solve the detrimental BS-

BS interference which affects cellular TDD systems. Thus, an ideal solution is one that does not explicitly make use of cell partitioning and that is not computationally complex.

FDD, in the classical sense (one frequency band for UL traffic and another for DL), does not effectively support channel asymmetry. TDD, on the other hand, is very well suited to support asymmetry since time resources can be distributed as per the asymmetry demands. Asymmetry in favour of DL results in an under-usage of the FDD UL band [8]. The idea presented in this work introduces an FDD-TDD switching point in the underused FDD band after which TDD is used to carry intra-cluster load. Thus, the FDD and TDD modes are combined in a soft manner.

Let a transmission slot be defined by a certain time duration and frequency allocation. A transmission slot can be considered as the basic building block of a duplex communication system. A series of alternating transmission slots (one transmission slot for UL and the next for DL) at different time instances but at the same frequency results in a pure TDD system. Two clumps of simultaneous transmission slots in opposing directions, one at a particular frequency and the other clump at a different frequency result in a pure FDD system. Introducing an FDD-TDD switching point in one of the frequency bands results in an FDD system before the switching point, a TDD system after the switching point and a simplex/broadcast transmission system in the other FDD band after the switching point. Fig. 1 makes this concept clearer. This, then, presents an efficient and elegant method of dealing with asymmetric traffic demands of users.

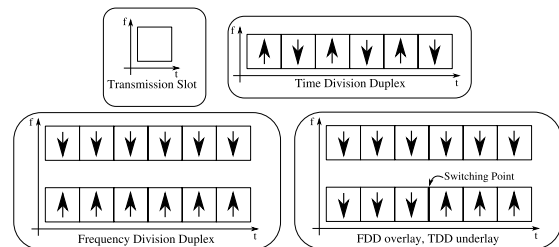


Fig. 1: A pure FDD system can be considered as two TDD systems without switching points. By eliminating the latter restriction, a whole class of new system designs are possible. Thereby, the advantages of both duplex modes can be exploited constructively while the disadvantages of each mode can be circumvented.

There is an increasing amount of research devoted to 3G femto-cells and home base stations [9] which are envisaged to reduce the load on macro-cell BSs and improve quality of service to indoor users. The usefulness of this scheme to femto-cell research is apparent due to the fact that no additional infrastructure or change in the air interface is needed.

Home networks are characterised by inter-communicating devices. A traditional FDD cellular system is incapable of supporting *ad hoc* communication between the entities of a cluster since all communication must be directed via the BS. The introduction of the TDD mode in the lesser used band enables *ad hoc* communication to take place within the cluster without over-burdening the BS.

The remainder of the paper is organised as follows. GM selection, frame structure, path loss and interference models are described in Section II. The simulation model is described in Section III. The metrics on which the system performance is evaluated are described in Section IV. The results are presented in Section V. Finally, Section VI includes concluding remarks and further work.

II. SYSTEM SETUP

A. Gateway Mobile

Practically, for the cluster to be formed, the MSs need to be aware of one another. One method of doing this is by making use of the receiver-initiated, time-multiplexed busy tone concept as described in [10], i.e., if the busy tone received by the GM of a cluster from a MS is above a pre-defined threshold, it belongs to the cluster.

One MS from each cluster of users is selected as a GM which relays traffic between the rest of the cluster and the BS (see Fig. 2).

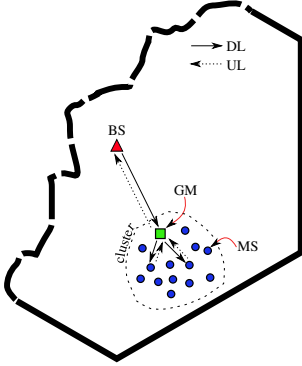


Fig. 2: Part of a cell showing one cluster. The GM acts as a relay between the BS and the other MSs in the cluster.

Introducing an additional hop in the system reduces the number of entities communicating with the BS since only one entity per cluster communicates with the BS, which leaves more resources for allocation per GM. Also, since transmission distances are reduced, higher signal-to-noise ratios (SNR) are available, leading to increased data-rates (especially within the cluster) through the use of higher order modulation schemes.

B. Frame Structure

Due to trends in user traffic requirements, it is assumed that all traffic in the system is asymmetric in favour of downlink. Therefore, the proposed frame structure allows for channel asymmetry in favour of DL. The unused resources in the FDD UL band are used for intra-cluster communication in the TDD mode.

The frame structure is as shown in Fig. 3. A frame consists of two chunks (a chunk is the basic time-frequency unit for resource-allocation), each of which consist of 12 OFDM symbols and 8 subcarriers. Since each chunk occupies a bandwidth of 312.5 kHz, the entire 50 MHz bandwidth (in UL and DL, each) can accommodate 160 chunks (512 subcarriers) with a subcarrier spacing of 39.0625 kHz. However, only 144 are available for use as the available bandwidth is 45 MHz (the rest being used up for guard bands) [11].

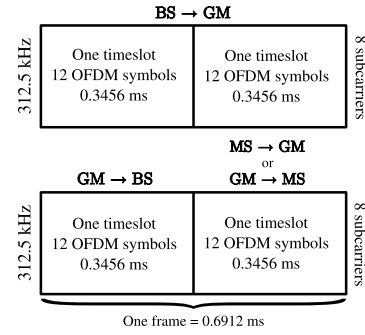


Fig. 3: The DL and UL frames, each with 2 chunks.

The entire DL band is dedicated to BS \rightarrow GM communication. In the UL band, in each frame, the first timeslot (TS) (with 144 chunks in the frequency domain) is reserved for GM \rightarrow BS communication and the second TS (again with 144 chunks) can either be used for GM \rightarrow MS or MS \rightarrow GM communication.

For the benchmark system, the same frame structure is used but without the TDD underlay. Therefore, the entire DL band is used for BS \rightarrow MS communication and the entire UL band is used for MS \rightarrow BS communication, thus resulting in a pure FDD system. Thus, in this case, the system does not provide support for asymmetric traffic and communication takes place over one hop.

C. Path Loss Model and Log-Normal Shadowing

For path loss calculations, WINNER path loss models are used [12]. Scenario C3 (metropol, bad urban macro-cell) is used for the macro-cell and scenario B3 (indoor hotspot) is used for the femto-cell (within the clusters). In both cases, the non line-of-sight equations are used in order to provide for the worst case scenario in terms of the desired link. The path loss models are of the form (obtained from [12])

$$PL[\text{dB}] = A \log_{10}(d[\text{m}]) + B + C \log_{10}\left(\frac{f_c[\text{GHz}]}{5}\right) + X, \quad (1)$$

where A , B and C are constants depending on the model used, f_c is the centre frequency depending on which band is being considered (this information is shown in Table I) and X is a normally distributed random variable with zero mean representing the shadowing component. For the B3 path loss model, $A = 37.8$, $B = 36.5$, $C = 23$ and standard deviation of the shadowing component $\sigma = 4$ dB. For the C3 path loss model, $A = 35.74$, $B = 42.61$, $C = 23$ and standard deviation of the shadowing component $\sigma = 6$ dB. It is ensured that the path loss between any two points does not fall below the free-space path loss which is calculated using

$$PL_{\text{free}}[\text{dB}] = 20 \log_{10}(d[\text{m}]) + 46.6 + 20 \log_{10} \left(\frac{f_c[\text{GHz}]}{5} \right). \quad (2)$$

In order to mimic realistic shadowing, a correlated log-normal fading model is implemented. Due to the slow fading process versus distance, adjacent fading values are correlated. The correlation in shadowing between two points separated by a distance Δx m is given by

$$R(\Delta x) = \exp \left(-\frac{\Delta x}{d_{\text{corr}}} \ln 2 \right), \quad (3)$$

where d_{corr} is the decorrelation distance (3 m for B3 and 50 m for C3) and represents the distance beyond which there is no correlation in shadowing [13].

D. Interference and SINR

The 144 available OFDM chunks are allocated equally to the GMs present in a cell (for UL and DL). The system does not make use of power control. Instead, each entity transmits with a fixed power, whose values are obtained from [11] (see Table I).

Four interference scenarios exist: $\text{GM} \rightarrow \text{BS}$, $\text{BS} \rightarrow \text{GM}$, $\text{GM} \rightarrow \text{MS}$ and $\text{MS} \rightarrow \text{GM}$. Same entity interference does not exist because the system is synchronised in time (crossed-slots do not exist). MSs of different clusters also do not interfere with one another because at any given time instant, all active MSs are either transmitting or receiving.

Both, co-channel interference (CCI) and multiple access interference (MAI) are considered. For the duration of the simulation, the channel is assumed to be static in time. However, frequency selective channels are simulated using Doppler shifts due to user mobility. MAI is not considered in the downlink (i.e., $\text{BS} \rightarrow \text{GM}$) since perfect synchronisation between subcarriers is assumed in the downlink.

MAI represents own cell interference and is modelled as the leakage from other subcarriers onto the set of subcarriers used by that particular entity. CCI represents other cell interference toward which all the subcarriers in the system contribute. Both, MAI and CCI, are calculated as shown in [14].

III. SIMULATION MODEL

The cellular scenario consists of 19 hexagonal cells in two tiers. Each cell, consisting of 3 sectors, contains a BS at its centre. A two-tier scenario consisting of hexagonal cells is used in the simulation. In order to mitigate the well-known

cell-boundary effect, a “dummy” four-tier system is generated for the same cluster density and the interfering effects of these entities are taken into account when calculating SINRs (signal-to-noise-plus-interference-ratio), thus ensuring that all users experience approximately the same amount of interference in the system.

The clustered distribution of users is simulated by uniformly distributed users within a circle. The clusters themselves are then uniformly distributed in the cellular scenario. It is assumed that for the duration of the simulation, the GM is idle, i.e., it does not receive or transmit any of its own data.

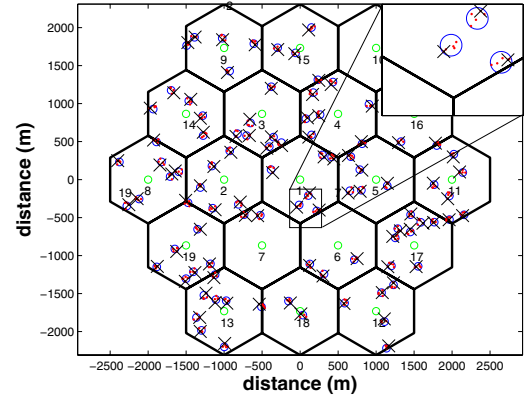


Fig. 4: One realisation of the clustered distribution for 100 clusters, each consisting of 4 MSs and a GM, uniformly distributed in a 2-tier scenario. The closeup shows 3 clusters with their respective selected GMs marked by crosses. The circles around the clusters (of radius 25 m) show the area within which the MSs of a cluster can be distributed. The circles at the centre of each cell show the locations of the BSs.

Every cluster is assumed to contain 5 MSs, one of which becomes the GM (see Fig. 4). One simulation snapshot is run for the duration of 8 frames such that every MS of a cluster is allocated 1 TS for UL and another for DL. In the TDD part of each UL frame, every GM communicates (either UL or DL) with one MS from the cluster. Thus, over the duration of the snapshot, there is duplex communication between the GM and every MS in the cluster. It is assumed that the MSs are static for the duration of the snapshot since the distance covered by a MS during the snapshot (considering approximately 3 km/hr mobility) is much less than the decorrelation distance of the path loss model and the snapshot duration is much shorter than the coherence time of the channel. The distribution of users is randomised for every snapshot as are the log-normal shadowing maps.

The parameters used in the simulation are summarised in Table I and are obtained from [11], [12], [15]. A best-effort system is simulated, i.e., full-buffer transmissions are assumed and capacities are calculated based on the achieved SINRs.

$$SE_{DL/UL} = \frac{\frac{TS_{DL/UL}^{BS-GM}}{TS_{avail}} \sum_{j=1}^{N_{GM}^{sys}} \sum_{i=1}^{N_C^j} \log_2 \left(1 + SINR_{i, DL/UL}^j \right) + \frac{TS_{DL/UL}^{GM-MS}}{TS_{avail}} \sum_{j=1}^{N_{MS}^{sys}} \sum_{i=1}^{N_C^j} \log_2 \left(1 + SINR_{i, DL/UL}^j \right)}{N_C \times N_{cells}} \quad (7)$$

TABLE I: Simulation Parameters

Parameter	Value
Simulation duration	5.5269 ms (8 frames)
Cell radius	577 m
Cluster radius	25 m
MSs per cluster	5 (including GM)
Mean user mobility	3 km/hr
Frequency offset	0% to 2%
Centre frequency in UL band (f_c^{UL})	3.7 GHz
Centre frequency in DL band (f_c^{DL})	3.95 GHz
Tot. BS Tx power	50.77 dBm
Tot. GM Tx power (to BS)	24 dBm
Tot. MS (and GM) Tx power (intra-cluster)	21 dBm
Tot. MS Tx power (benchmark system)	24 dBm
Antenna elevation gain	14 dBi

IV. PERFORMANCE METRICS

The capacity (per frame) achieved on a link k is calculated as shown in (4)

$$C_k = \frac{TS^k}{TS_{avail}} W \sum_{i=1}^{N_C^k} \log_2 \left(1 + SINR_i^k \right), \quad (4)$$

where W is the subcarrier bandwidth, N_C^k represents the number of subcarriers allocated for link k , $SINR_i^k$ is the SINR achieved on the i^{th} subcarrier on the k^{th} link, TS^k represents the number of TSs used for link k and TS_{avail} is the total number of TSs used in the simulation.

The capacity gain due to intra-cluster communication is defined as the ratio of the capacity between GMs and their MSs to the capacity achieved between the BSs and MSs in the benchmark system as shown in (5)

$$G = \frac{C_{GM \leftrightarrow MS}}{C_{BS \leftrightarrow MS}^{bench}}, \quad (5)$$

where $C_{GM \leftrightarrow MS}$ is the mean capacity between the GMs and their associated MSs and $C_{BS \leftrightarrow MS}^{bench}$ is the end-to-end capacity in the benchmark system.

The normalised system spectral efficiency is defined as the system spectral efficiency normalised by the number of cells and subcarriers available. For the benchmark, this spectral efficiency is calculated as shown in (6)

$$SE_{DL/UL}^{bench} = \frac{\sum_{j=1}^{N_{MS}^{sys}} \sum_{i=1}^{N_C^j} \log_2 \left(1 + SINR_{i, DL/UL}^j \right)}{N_C \times N_{cells}}, \quad (6)$$

where N_{MS}^{sys} is the number of MSs in the system, N_C^j is the number of subcarriers allotted to the j^{th} MS, N_C is the total number of subcarriers available and N_{cells} is the number of cells in the system.

In the proposed system, the system spectral efficiency is the sum of the spectral efficiencies achieved on the BS-GM link and the GM-MS link. This is calculated as shown in (7). Here, N_{GM}^{sys} is the number of GMs in the system, $TS_{DL/UL}^{BS-GM}$ is the number of TSs allocated to any BS-GM link for the simulation (this is 16, all the available TSs for DL and 8 for UL) and $TS_{DL/UL}^{GM-MS}$ is the number of TSs allocated for GM-MS communication which is 1 for either UL or DL.

V. RESULTS

Fig. 5 shows the capacities achieved on average for a GM-MS pair. At any time instant, only one entity in every cluster is active. All entities within a cluster transmit at the same power. Since the MSs within a cluster are geographically concentrated, they undergo similar shadowing on average, which leads to the interference being very similar across time slots. As a result, due to this and channel reciprocity, the UL and DL capacities show nearly identical trends. As the number of clusters is increased, due to increased interference (CCI), the capacities decrease.

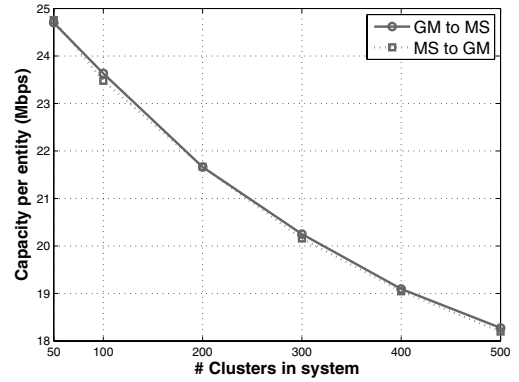


Fig. 5: Mean achieved capacity between GMs and their associated MSs. As the number of clusters is increased, higher interference leads to reduced capacities.

Fig. 6 shows the capacity gain due to intra-cluster communication as described by (5). It is seen that the capacity gain increases as the number of clusters in the system is increased. This is because the capacity between GMs and their MSs does not decrease as fast as the capacity between the BSs and MSs in the benchmark system as the number of clusters in the system is increased. Furthermore, it is seen that the gain in UL is higher than that in the DL. This is because the UL capacity in the benchmark system is affected by MAI which is not the case in the DL. This causes the UL capacity in the benchmark system to be lower than the DL capacity which translates to the capacity gain being higher in UL. The difference between

the UL and DL gains reduces as the number of clusters is increased because the difference between the UL and DL capacities in the benchmark system grows smaller with an increasing user density.

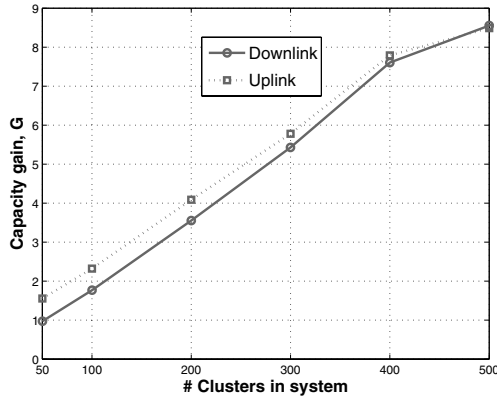


Fig. 6: Gain in capacity through the use of intra-cluster communication.

Finally, Fig. 7 shows the system spectral efficiencies in the proposed and benchmark systems as described in (6) and (7). It is clearly seen that the proposed and benchmark systems display opposing trends. In the benchmark system, the spectral efficiency decreases with increasing number of clusters in the system. This is due to the fact the interference is increased with an increasing user density which causes the SINRs of the subcarriers to decrease, which eventually leads to a decrease in system spectral efficiency. The TDD underlay with intra-cluster communication results in an increase in system spectral efficiency because in this case, the spectral efficiency is the sum of spectral efficiencies on the BS-GM hop and the GM-MS hop. The SINRs on the GM-MS link are much higher compared to the BS-GM link (due to shorter transmission distances) and the entire bandwidth is used within a cluster. Therefore, an increase in the number of clusters in the system results in an increase in the system spectral efficiency.

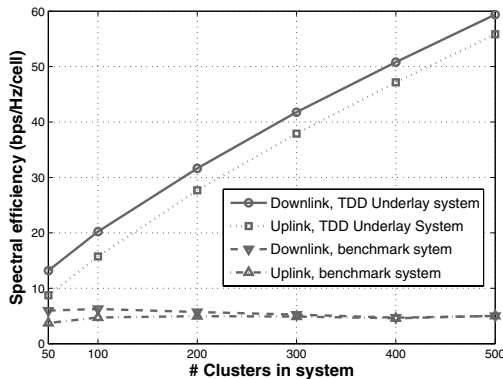


Fig. 7: Spectral efficiencies in the proposed and benchmark systems.

VI. CONCLUSION AND OUTLOOK

This paper presents a method of introducing a TDD component to an FDD system, thereby enabling *ad hoc* communication to take place between the entities of a cluster without overburdening the BS. *Ad hoc* communication between devices in close vicinity of one another is an envisaged characteristic of so-called home networks or femto-cells. Results show that this type of “intra-cluster communication” can be supported through the use of the TDD underlay concept without adding any infrastructure to a cellular system.

Merging of closely situated clusters into a single cluster such that the system supports clusters with varying number of users, introduction of power control and link adaptation are areas of further research.

ACKNOWLEDGMENT

This work was supported by DFG grant HA 3570/2-1 as part of program SPP-1102 (Adaptability in heterogeneous communication networks with wireless access - AKOM).

REFERENCES

- [1] M. Flament, F. Gessler, F. Lagergren, O. Queseth, R. Stridh, M. Unbe-daun, J. Wu, and J. Zander, “An Approach to 4th Generation Wireless Infrastructures-Scenarios and Key Research Issues,” in *Proceedings of the 49th IEEE Vehicular Technology Conference (VTC)*, vol. 2, Amsterdam, Netherlands, May 16–20 1999, pp. 1742–1746.
- [2] P. Jain, H. Haas, and S. McLaughlin, “Capacity Enhancement Using Ad Hoc Pico-Cells and TDD Underlay,” in *Proceedings of the 17th IEEE International Symposium on Personal, Indoor and Mobile Radio Communications (PIMRC)*, Helsinki, Finland, September 11–14 2006, pp. 1–5.
- [3] H. Claussen, “Distributed Algorithms for Robust Self-deployment and Load Balancing in Autonomous Wireless Access Networks,” in *IEEE International Conference on Communications (ICC)*, vol. 4, Istanbul, Turkey, June 11–15 2006, pp. 1927–1932.
- [4] H. Y. Hsieh and R. Sivakumar, “Performance Comparison of Cellular and Multi-Hop Wireless Networks: a Quantitative Study,” *SIGMETRICS Performance Evaluation Review*, vol. 29, no. 1, pp. 113–122, 2001.
- [5] H. Wu, C. Qiao, S. De, and O. Tonguz, “Integrated Cellular and Ad Hoc Relaying Systems: iCAR,” *IEEE Journal on Selected Areas in Communications*, vol. 19, no. 10, pp. 2105–2115, Oct. 2001.
- [6] A. N. Zadeh, B. Jabbari, R. Pickholtz, and B. Vojcic, “Self-Organizing Packet Radio Ad Hoc Networks with Overlay (SOPRANO),” *IEEE Communications Magazine*, vol. 40, no. 6, pp. 149–157, June 2002.
- [7] K. M. Koumadi and Y. Han, “TDD Time Slot Allocation and Interference Analysis for HDD Cellular Systems,” in *Asia-Pacific Conference on Communications (APCC)*, Busan, Korea, August 31 – September 2 2006, pp. 1–5.
- [8] H. Haas and G. J. R. Povey, “A Capacity Investigation on UTRA-TDD Utilising Underused UTRA-FDD Uplink Resources,” in *IEEE Colloquium on UMTS Terminals and Software Radio (Ref. No. 1999/055)*, Glasgow, Scotland, April 1999, pp. 1–7.
- [9] H. Claussen, L. T. W. Ho, and L. G. Samuel, “Financial Analysis of a Pico-Cellular Home Network Deployment,” in *IEEE International Conference on Communications (ICC)*, Glasgow, Scotland, June 24–28 2007, pp. 5604–5609.
- [10] H. Haas, V. D. Nguyen, P. Omiyi, N. Nedev, and G. Auer, “Interference Aware Medium Access in Cellular OFDMA/TDD Networks,” in *IEEE International Conference on Communications (ICC)*, vol. 4, Istanbul, Turkey, June 11–15 2006, pp. 1778–1783.
- [11] IST-4-027756 WINNER II, “D6.13.7, WINNER II Test Scenarios and Calibration Cases issue 2,” Retrieved March 15, 2007, from <https://www.ist-winner.org/WINNER2-Deliverables/>, December 2006.
- [12] IST-4-027756 WINNER II, “D1.1.2 v1.0 WINNER II Channel Models,” Retrieved October 18, 2007, from <https://www.ist-winner.org/WINNER2-Deliverables/>, September 2007.
- [13] ETSI 30.03 TR 101 112 v3.2.0, “Selection Procedures for the Choice of Radio Transmission Technologies of the UMTS,” Sophia Antipolis Valbonne, France, 1998.
- [14] E. Foutekova, P. Agyapong, and H. Haas, “Channel Asymmetry and Random Time Slot Hopping in OFDMA-TDD Cellular Networks,” in *Proceedings of the 67th IEEE Vehicular Technology Conference (VTC)*, Marina Bay, Singapore, May 11–14 2008, pp. 5 pages on CD-ROM.
- [15] IST-2003-507581 WINNER, “D7.2 WINNER System Assessment Criteria Specification,” Retrieved October 18, 2007, from <https://www.ist-winner.org/DeliverableDocuments/>, July 2004.